Reversible thermochromic Cobalt(II) coordinated malonic acid/nanocellulose hybrid aerogels as a humidity sensor

or

Cobalt(II) coordinated malonic acid/nanocellulose hybrid aerogels exhibiting reversible thermochromism

Hasna M. Abdul Hakkeem [†,‡], *Ardra V.S.* [†], *Adrija De* [†], *M. Padmanabhan* [§], *Saju Pillai* [†,‡,*]

[†] *Materials Science and Technology Division, CSIR-National Institute for Interdisciplinary Science and Technology (CSIR-NIIST), Thiruvananthapuram - 695019, Kerala, India*

[‡] *Academy of Scientific and Innovative Research (AcSIR), Ghaziabad - 201002, India*

[§] *Department of Chemistry, Amrita university, Amrithapuri, Kollam- 690525, Kerala, India*

* Corresponding author.

E-mail: pillai_saju@niist.res.in (S. Pillai)

ABSTRACT

Growing global interest in sustainability always attracted to 'nanocellulose' as a green candidate in vast areas of applications. Here we report Co^{2+} cation induced malonic acid/nanocellulose aerogels that shows reversible thermochromism. Since transition from tetrahedral to octahedral geometry upon the interaction with water molecules in the moisture is behind this thermochromism. High surface area behaviour of aerogel structures make this phenomenon more enhanced. Co(II) ions and malonic acid as components ensured the coordination and crosslinking functions by employing interactions with extrinsic number of functional groups in TEMPO-oxidised cellulose nanofibers (TCNF) leads to the formation of hierarchically porous aerogel structures. Detailed characterisations of synthesised aerogels were carried out to evaluate the overall properties and performance. Reversible thermochromism performance of this hybrid aerogels were utilized for visible humidity sensing

designing an android application. This green pathway of aerogel formation can be adopted for many vast areas with diverse metal ions and additives upon requirements.

KEYWORDS:

Thermochromic aerogels, reversible thermochromism, TEMPO-oxidised cellulose nanofibers (TCNF), Co(II)/nanocellulose hydrogel, Co(II)/ nanocellulose aerogels, Co(II)/ malonic acid/nanocellulose hybrid aerogels, Humidity sensing

INTRODUCTION

Time to choose green and biodegradable polymer materials instead of the sources of most of the white pollution that is petroleum based polymers is already past. Cellulose as most abundant semi-crystalline natural polymer but its utility is always pressed down by its poor processibility and compactability. Arrival of the nano prototype of cellulose with variant functionalities named as 'nanocellulose' made a huge turn to the road to the uncountable applications of this sustainable material.[1] Lot of researchers are worshipping in this area to spread this network of nanocellulose materials in mesmerizing outlooks for innovative ideas. These outlooks include photonic materials,[2] flexible films,[3] packaging materials,[4] hydrogels,[5] aerogels,[6] fibers,[7] biomedical scaffolds [8] etc.

TEMPO- oxidised nanocellulose fibers, a sub division of nanocellulose materials are born with ultra-aqueous stability in nano-level imparted by the inter and intra molecular hydrogen bonds, and induced carboxyl functionalization proven by a zeta potential of about -70 mV.[9] Thixotropic behaviour of nanocellulose especially cellulose nanofibers (CNF) even in low concentrations always delivered the signal for the applicability of this sustainable materials in the realm of hydrogels and aerogels with its significant asset like entangled fibrous structure with high aspect ratio.[10] This important property can be successfully tuned and transforms in to a stable hydrogel by impregnating metal cations especially divalent metal cations in to the nanocellulose hosting matrices.[11] Both induced carboxyl and inherent hydroxyl groups of nanocellulose fibers enables the distribution of the metal ions homogeneously throughout the network by coordination followed by immediate transformation into hydrogel. Metal ions coordinated nanocellulose stable hydrogels can be captured into light weight aerogels by different cryogenic drying processes. Only few appreciable research attempts are there to fabricate fast hydrogels of TEMPO- oxidised nanocellulose by incorporating metal ions by coordinating with carboxyl functional groups. Zander et al., demonstrated the fabrication of

Ca^{2+} and Fe^{2+} cross linked cellulose nanofiber hydrogels for tissue engineering applications.[11a] Hai et al., reported the latent fingerprint detection and encryption using luminescent Tb^{3+} nanocellulose complex hydrogels.[11b] Dong et al., also discussed Ca^{2+}, Zn^{2+}, Cu^{2+}, Al^{3+}, and Fe^{3+} intermediated hydrogelation of entangled TEMPO-oxidised cellulose nanofibers in detail.[12] The properties homogeneity and strong binding of this nanocellulose metal ions hybrid gels can be upgraded by the addition of simple organic dicarboxylic acids like malonic acid, maleic, oxalic, and succinic acid etc. Surprisingly, these combinations than can trigger the overall properties of metal ions induced nanocellulose gels has rarely been can explored in the literature.

Thermochromic materials are unique and invariant thermoreponsive matrials that change its colour to another and have been widely applied in areas such as temperature sensors, anti-counterfeiting, modern electronic devices etc.[13] If the thermochromic material is reversible it can owe to more sacksful applicability in various fields. Nanocellulose can act as a successful hosting matrix in different physical appearances such as films, gels etc. to thermochromic materials towards novel applications. Recently, Jaiswal et al., reported creating thermoresponsive devices by incorporating black thermochromic pigment for optical modulation device.[14]

Humidity sensors are important category of sensors that can make a huge impact in the agricultural, food processing and pharmaceutical industry.[15] A variety of humidity sensors are available in market and new products are arises day by day with fascinating features and improved efficacies.[16] Even though ideal capabilities of a humidity sensor needs to be more improved in terms of its sensitivity, less response and recovery time, eco-friendliness thermal stability etc. Ceramics, organic polymers and inorganic-polymer hybrids are the main rulers in this realm of humidity sensors.[17] Cobalt based metal organic frame work (MOFs) are recent inmates in the humidity sensor economy by the inherent visual colour based humidity sensing property of Cobalt metal.[18] Colourimetric change arises through the change in coordination number of Co(II) with the H_2O in moisture as a ligand is behind this visual magic treat.[17] Co(II) based MOFs can act as vital determinant in the efficiency of humidity sensors whereas poor processibility of MOFs always become hurdle for the designing and practical applicability of humidity sensor devices. Comparing with the above mentioned common ceramic humidity sensors especially porous silica based materials are well known because of their surface area, pore size and distribution.[19] Even though these pore structures are well suitable to provide more

binding sites for water molecules, recovery time of ceramic based humidity sensors are too long.[20] Since polymer based materials are popular for light weight and more flexible with better mechanical properties these features can provide more merits to the polymer based humidity sensor products but suffers from slow response.[17] This limitation of polymer based humidity sensors can be covered by impregnating Co(II) and surface area and porosity of ceramic humidity sensors can be achieved by aerogel structure nanocellulose. In addition, comparing to dense solid material substrates, aerogels known by 99% air contact can show more accessibility to the water molecules to the fifth and sixth free coordination sites of Co(II) by the surface area and porosity.

In this paper, we report a sustainable synthetic strategy for Co(II) coordinated malonic acid/nanocellulose hybrid aerogels that shows interesting property of thermochromism. Water molecules in the moisture plays a key role in this Co(II) based system and hence this property of reversible thermochromism can be tuned and utilized towards humidity sensing. The novelty of this work is the different approach the modified the comprehensive properties of Co(II) coordinated nanocellulose aerogels by adding a simple dicarboxylic acid, malonic acid as an additive. To the best of our knowledge, this combination of three distinct components has never before been documented in the literature for applications like humidity sensing. We also tried to demonstrate the real life applicability of this humidity sensing material by developing a specific and robust android application.

The novelty of this work is the unique approach that modified the comprehensive properties of Co(II) coordinated nanocellulose aerogels by incorporating a simple dicarboxylic acid, malonic acid, as an additive.

EXPERIMENTAL SECTION

Materials. Chemically treated (sodium hydroxide, NaOH) banana pseudo-stem fibers were used as cellulose source. Sodium chlorite ($NaClO_2$), 2,2,6,6-tetramethyl piperidine-1-oxyl radical (TEMPO; $C_9H_{18}NO$), sodium hypochlorite (NaClO), sodium hydroxide (NaOH), sodium bromide (NaBr) used for oxidation of the cellulose prior to ultrasonication to cellulose nanofibers were purchased from Sigma-Aldrich, India. Cobalt(II) acetate anhydrous ($C_4H_6CoO_4$) (98%) was purchased from Alfa Aesar and malonic acid ($C_3H_4O_4$) was from Sigma-Aldrich. All other chemicals, such as sodium hydroxide (NaOH), hydrochloric acid (HCl), lithium chloride (LiCl), magnesium chloride ($MgCl_2$), magnesium nitrate ($Mg(NO_3)_2$), Sodium chloride (NaCl), potassium chloride (KCl), potassium sulphate (K_2SO_4) were of analytical grade. Ultrapure deionized (DI) water (Milli-Q purifier system, Merck, Germany) was consumed as solvent in the complete synthesis procedure and tert-butanol ($C_4H_{10}O$) was utilized for washing procedure.

Preparation of TEMPO-Oxidised Cellulose Nanofibers (TCNF).

Same typical protocol of TEMPO-oxidation for the synthesis of TEMPO-oxidised nanocellulose described elsewhere was adopted, by only choosing homogenization instead of ultra-sonication to obtain fibers.[21] The whole reaction system was transferred to the homogenizer only for a one pass at 50 MPa. The gel like product obtained was thoroughly washed and stored at 4 ^{o}C in wet conditions for further modifications.

Synthesis of Cobalt(II) Induced Malonic acid/Nanocellulose Hybrid Aerogels (CoMNC).

A mixture 3 mL of 0.033 g malonic acid and 1.5 wt% nanocellulose dispersion was taken in a cultural tube. Instant white color gel formed by the shaking was incubated in an aqueous solution contains almost 0.063 g of cobalt acetate for 24 h. The obtained pink color mechanically stable hydrogels were placed in a preheated oven at 90 ^{o}C for 10 min followed by washing thoroughly with water, water: tert-butanol mixture to exchange the solvent to t-BuOH followed by freeze-drying. The resultant violet color aerogels were termed as CoMNC aerogels. As well as aerogels fabricated by simply mixing similar amount of cobalt acetate to nanocellulose dispersion without malonic acid also demonstrated in the same procedure as control sample were denoted as CoNC.

pink-colored

remove as well as

put comma

Methods.

Physical Characterization of Aerogels.

The carboxyl content of TCNF were determined by standard conductometric titration on lab scale. O/C ratio and chemical states of TCNF samples, CoMNC, and CoNC aerogels were evaluated employing X-ray photoelectron spectroscopy (XPS) by PHI 5000 VersaProbe II, ULVAC-PHI Inc., USA. FTIR spectroscopic transmittance of samples were recorded from PerkinElmer FTIR spectrometer in the 4000-500 cm^{-1} region operated at a resolution of 4 cm^{-1} and 16 scans. Particle distribution by dynamic light scattering (DLS) and zeta potential of TCNF were studied by accessing Zetasizer Nano ZS, Malvern equipment using a sample concentration of 0.1 % (w/v). Morphology of TCNF was monitored by Atomic force microscopy (AFM) by Multimode 8 atomic force microscope; Nanoscope V controller (Bruker, Santa Barbara, CA) under tapping mode. Samples for AFM were prepared by coating and drying TCNF dispersion over mica sheet as substrate. PANalytical X'pert pro equipped with Cu Kα (λ=1.54 Å), 45 kV is being used to obtain powder X-ray diffraction (XRD) pattern of

all samples. Scanning electron micrographs were acquired by subjecting fraction of aerogel samples to Zeiss EVO 18 cryo-SEM at 15 kV. Density of aerogels samples were formulated from mass by volume ratio. Nitrogen adsorption−desorption studies were performed to find out Brunauer-Emmett-Teller (BET) surface area and Barrett-Joyner-Halenda (BJH) pore-size distributions using Gemini 2375, Micromeritics, Norcross, USA. A minimum 12 h of degassing prior to surface area studies of aerogels is required. Thermogravimetric analysis (TGA) analysis were conducted with simultaneous thermogravimetric analyzer (STA 7300, Hitachi, Japan) in the range from 50 to 700^{o}C at a rate of 5 °C/min in the air. Mechanical specifically compression strength of aergel samples were evaluated by a universal testing machine (Hounsfield, H5KS UTM, Redhill, U.K.); crosshead speed- 1.0 mm min^{-1}. UV- visible absorption maxima of CoMNC aerogel samples were measured from UV-Visible spectrophotometer (Shimadzu UV-2700, Shimadzu, Japan).

Formulation of Humidity Sensor Android Application.

Humidity sensor android application was developed by programming in Java and edited using Android studio as IDEs an IDE (integrated development environment). The application designing detail is shown in (Supporting Information). Visible light spectrum corresponding to λ_{max} obtained from UV-Visible absorption spectroscopy of CoMNC samples at different humidity environment were collected and utilized as input in the programming. Standard and known humidity environment were created in glass desiccators having saturated LiCl, $MgCl_2$, $Mg(NO_3)_2$, NaCl, KCl, and K_2SO_4 solutions, which provides the humidity levels of 11%, 33%, 53%, 75%, 85%, and 97%, respectively.[22] Absorption maxima (λ_{max}) were recorded at 25^{o}C and relative humidity of 50-52%.

RESULTS AND DISCUSSION

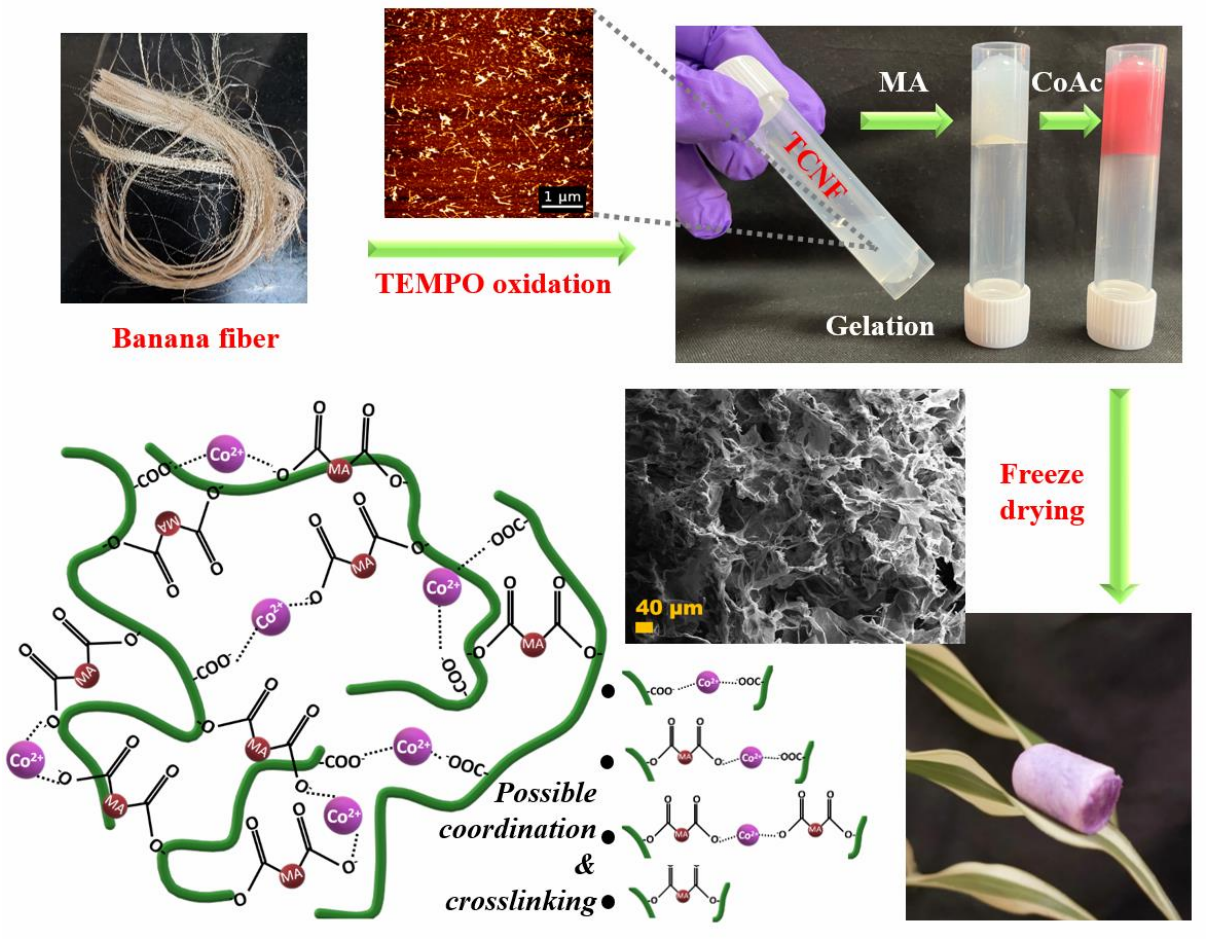

Scheme 1. Synthesis of Cobalt(II) coordinated malonic acid/nanocellulose hybrid aerogels and schematic illustration of possible coordination and crosslinking in the formed aerogels.

TEMPO-oxidation is desirable in the fabrication of metal ion coordinated aerogels since it evokes the carboxyl functionalization in cellulose that ensure the coordination with metal ions. According to the experimental section, TEMPO-oxidation followed a mild homogenization process to exfoliate cellulose nanofibers (TCNF) from banana pseudo-stem fibers. After being oxidized by TEMPO mediated oxidation, C6 hydroxy groups of cellulose selectively will convert into carboxyl group which is determined to be 1.06 mmol/g by conductometric titrations and an O/C ratio of about 0.6 was obtained from XPS analysis which is higher than that for holocellulose (O/C ratio= 0.41) from banana pseudo-stem fibers. Qualitative confirmation of introduced carboxyl groups in cellulose is done with FTIR analysis and confirmed from the new sharp peak arise at 1600 cm^{-1}.[23] Electrostatic repulsions between the carboxyl groups and inter and intra molecular hydrogen bonding will always provide stable aqueous suspensions of TCNF as shown by the value of the zeta potential, -60.02 mV. Size distribution and morphology of TCNF were confirmed by AFM and DLS analysis (Figure S1).

will convert --> converted to

Visual detection of morphology of TCNF were done using AFM in tapping mode. Figure S1a, the AFM height image, depicts the development of individual fibers having width, 15 ± 2 nm and width, and length of few hundred nanometers according to the high aspect ratio of cellulose nanofibers. Peak in the size distribution pattern located at 390 to 830 nm region having an average particle size as 612 nm with a PDI of 0.2 gave information about the fibrous structure of TEMPO-oxidized nanocellulose with almost uniform size (Figure S1b).

Fluidity of 1.5 wt% TCNF dispersion was discarded by the addition of anhydrous Co (II) acetate salt denoted as CoNC. This rapid gelation is happened due to the bonding affinity of metal in +2 oxidation states to the carboxyl groups induced by the TEMPO oxidation in TCNF. Hence the strength of hydrogels will ultimately depend upon the degree of carboxylation in TCNF which will vary by several factors including source of cellulose.[24] As a preliminary step put comma we added 1.2 M anhydrous cobalt acetate to 1.5 wt% TCNF suspension and mixed in a vertex mixer for 30 s and denoted as CoNC. After instant mixing put comma there is small extent of fluidity and inhomogeneity in the physical appearance of pink hydrogel was observed. Even though complete gel formation was observed after 24 h put comma homogeneity was not attained. Even though some literature discussed instant homogeneous gel formation with other metal ions like Ca^{2+}, Fe^{2+}, Al^{3+}, Cu^{2+} put comma etc. our experiments gave the thought that this phenomenon is purely based on the degree of carboxylation which may change even by personal experimental errors.[11-12] So another alternative options are needed in such cases to form an ultra-stable and sustainable hydrogels. Adding ligands that can form MOF with Cobalt is one option and it has been employed employed by several researchers.[6] But these ligands are expensive and toxic in nature. Selective and versatile functionalization of nanocellulose with carboxyl groups enabled enables the binding of metal ions to the sustainable nanocellulose matrix and resulted in to rapid build mechanically stable aerogels. In addition to TEMPO-oxidation, formation of semi-acid esters resulted from the reaction of cellulose with polycarboxylic acids or their derivatives is an alternative or additional pathway to increase the carboxylic contents to an extent. Among the organic polycarboxylic acids, dicarboxylic acids are potential candidates to form an ester linkage between hydroxy groups of cellulose and one carboxyl group with the other end carboxyl group remaining free. Under some conditions these free carboxyl ends of dicarboxylic acids also react with the cellulose hydroxyl groups and gave cross- linkage between cellulose chains.[25] Cross linking of cellulose chains can be utilized in mechanical strength of nanocellulose based hydrogels and aerogels to an extend where as whereas concerned maximization of cross linking without free carboxyl groups can be hindered in presence of Co^{2+} metal ions and water as solvent in the system. Dicarboxylic

acids like citric acid, malonic acid and maleic acid etc. are also recognized by the researchers as organic acid catalyst for the exfoliation of nanocellulose fibers from holocellulose at optimum reaction conditions.[26] These optimum conditions includes high acid concentration, elevated temperature etc., that minimize cellulose crosslinking acids and acids can be recovered after the reaction.[26b] Selection of malonic acid as the organic carboxylic acid in the development of mechanically stable Co^{2+} coordinated nanocellulose aerogels raised the coordination affinity of Co^{2+} with malonic acid and also the less possibility of effective cross linking by the second carboxyl group of dicarboxylic is very less compared to the crosslinking efficiency of polycarboxylic acids.[27] Main five types of possible chemical interactions in the Co^{2+} induced malonic acid/nanocellulose aerogels (CoMNC) includes coordination between two carboxyl groups of TCNF formed by TEMPO oxidation and Co^{2+} ion (TCNF-COO^-…Co^{2+}…$^-$OOC-TCNF), coordination between one carboxyl group of TCNF formed by TEMPO oxidation and one free carboxyl end of semi acid ester of cellulose made by the malonic acid with Co^{2+} ion (TCNF-COO^-…Co^{2+}…$^-$OOC-CH_2-COO-TCNF) , two free carboxyl end of semi acid ester of cellulose made by the malonic acid and Co^{2+} ion (TCNF-COO-CH_2-COO^-…Co^{2+}…$^-$OOC-CH_2-COO-TCNF) and the last one is cross linking between cellulose chains by malonic acid as depicted in scheme 1. Coordination between Co^{2+} and two carboxyl groups of same malonic acid or different malonic acid is negligible here hence it will form insoluble coordination crystal forms (MOFs) in aqueous media depending upon the severity of reaction conditions.

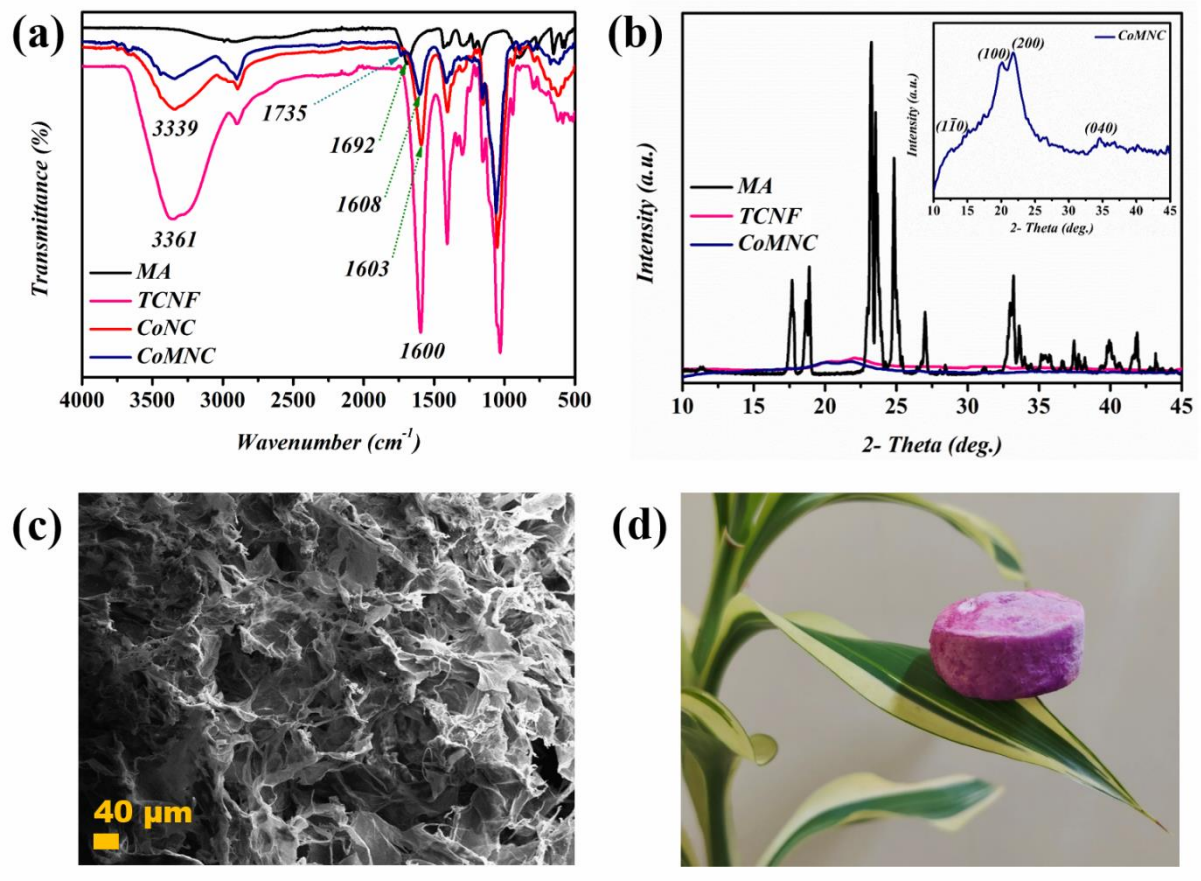

Figure 1. (a) FT-IR spectra, (b) PXRD of malonic acid (MA), TEMPO-oxidised nanocellulose (TCNF), CoNC and CoMNC aerogels, (c) SEM micrographs and (d) physical appearance of fibrous CoMNC aerogels.

FT-IR spectra of MA, TCNF, CONC and CoMNC aerogels were collected to evaluate the interaction between carboxylated nanocellulose, MA and Co^{2+} ions (Figure 2a). TEMPO-oxidised cellulose nanofibers showed a peak at 1600 cm^{-1} that typical for the carboxyl group. In the FT-IR spectra of CoNC aerogels shows a narrow shift in the peak corresponding to carboxy groups to 1603 cm^{-1}. After the formation of aerogel with MA and Co^{2+} ions, this peak underwent a high frequency shift to 1608 cm^{-1} with an additional peak at 1735 cm^{-1}. This shift happened by coordination of carboxyl groups with the metal ions. This small new-born peak at 1735 cm^{-1} validates the formation of ester groups in the system to some extent that theoretically has vibration peak at higher frequency than the carboxylic acids.[28] While considering the –OH stretching vibration peak of nanocellulose at 3361 cm^{-1} got broadened, was observed
low- frequency shift with a significant decrement in the intensity. This characteristic change can be explained by the coordination of numerous –OH groups of cellulose with cobalt ion which impart a cross-linked gel morphology.[6] And utilization of hydroxy groups of cellulose

for the formation of semi acid ester of cellulose also in agreement with noticeable decrement in the –OH symmetric stretching peak intensity. The absorption bands between 500 and 700 cm^{-1} can be identified of M-O bonds on the sample which were observed in both TCNF and CoMNC resulted from the COO---Na^{+} in TCNF and COO---Co^{2+} coordination interactions in CoMNC respectively. Overall information obtained from FT-IR spectra of variant samples qualified the formation of different coordination interactions and cross linking mentioned above, which are possible behind the formation of stable CoMNC aerogels. PXRD patterns of MA, TCNF and CoMNC aerogels were presented in Figure 2b. Typical XRD patterns of cellulose II contains characteristic peaks at $2\Theta = 12.6^{o}$, 20.03^{o}, and 21.89^{o} corresponding to the planes (1− 10), (110) and (200), respectively. PXRD pattern of CoMNC aerogels obtained was exactly similar to the diffraction pattern of cellulose II and great difference from the PXRD pattern of MA crystals. These PXRD observations illustrated that MA must be reacted with TCNF and Co^{2+} ions and malonate moiety must be introduced into amorphous coordinated polymer form successfully and no cobalt malonate MOFs are formed. CoMNC aerogels have irregularly shaped and sized pores as shown in the SEM image (Figure 1c) created by the layered sheets like structures of assembled cellulose nanofibers cross-linked by MA and Co^{2+} ions. The CoMNC aerogels formed were structurally strong and light weight having a density of about 0.04 g/cm^{3} (Figure 1d).

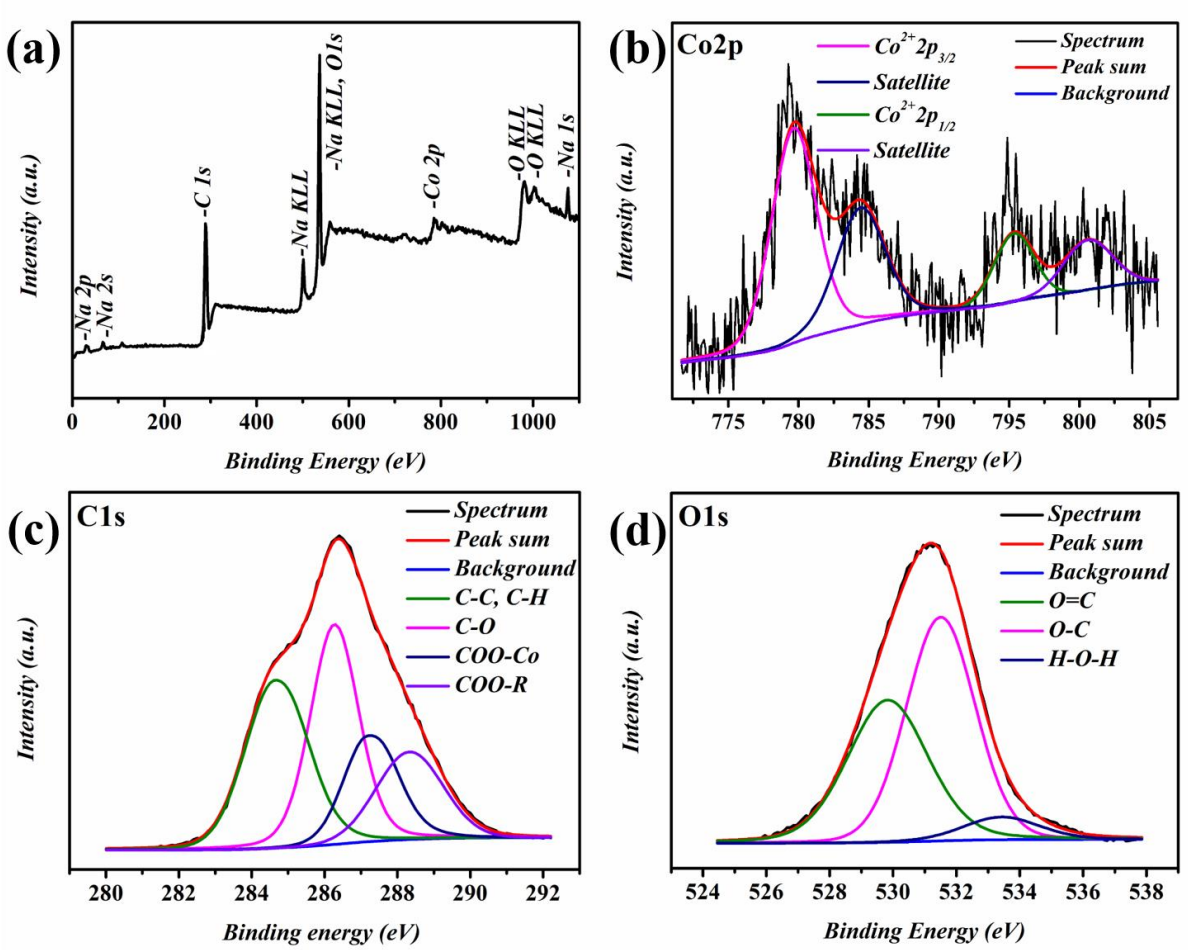

Figure 2. (a) survey, deconvoluted XPS spectra of (b) Co2p, (c) C1s and (d) O1s of CoMNC aerogels.

In order to examine the chemical states of elemental constituents of CoMNC aerogels, XPS analysis were done and resultant survey spectrum shows the major elemental constituents of aerogels as Co, O, C and some amounts of Na that arises in the TCNF from different stages of exfoliation of nanocellulose from plant source (Figure 2a). XPS spectra was deconvoluted for Co2p, C1s and O1s as represented in Figure 3b, c, and d. Prominent Co2p core level signal contained two coexhibited doublets corresponding to Co^{2+} species (Co^{2+} 2p3/2 at 779.9 and Co^{2+} 2p1/2 at 795.2 eV with a spin-orbital splitting of ~15.4 eV), satellite peaks (784.5 and 800.6 eV) respectively.[29] Figure S2 shows the deconvoluted Co2p spectra of CoMNC aerogels along with the Co2p spectra of CoNC, control samples synthesised in absence of malonic acid for comparison. Co2p in CoMNC has shifted to a lower binding energy compared to corresponding in CoNC, this shift indicates that electronic or coordination interactions between the Co^{2+} ions and the supporting matrix is turned to more strong.[30] These corroborate the necessity of malonic acid in the formation of this mechanically stable CoMNC hydrogels and

aerogels. Deconvoluted XPS spectra of C1s for CoMNC found to be entirely different in proportions of all four distinct peaks for characteristic bonds from usually obtained C1s spectra for purely TEMPO-oxidised nanocellulose based systems envisaged the presence of malonic acid also in the backbone aerogel scaffold.[31] Distinct peak at 287.02 eV signifies the strong coordination between Co^{2+} ions (metal ions) and carboxyl groups in the TCNF/MA template.[31] The noticeable peak at 288. 32 eV can be assigned to ester moiety formation in CoMNC and it cannot be able to differentiate from that for TCNF since free COOH groups will also shows show peak in these region of C1S XPS spectra.[28] However, increment in the intensity of this peak is considerable. The O1s spectrum can be decomposed in into three distinct peaks at 529.81 (O=C), 531.50 (O-C), and 533.48 eV (absorbed H_2O), respectively. Low shift in the O1s characteristic peaks strongly promoted the fact of strong interaction between oxygen and metal present in the system (Figure S3). In addition, the appearance of a peak at 533. 48 eV, which was assigned to absorbed water molecules, was observed and is not always found in O1s spectra.[32]

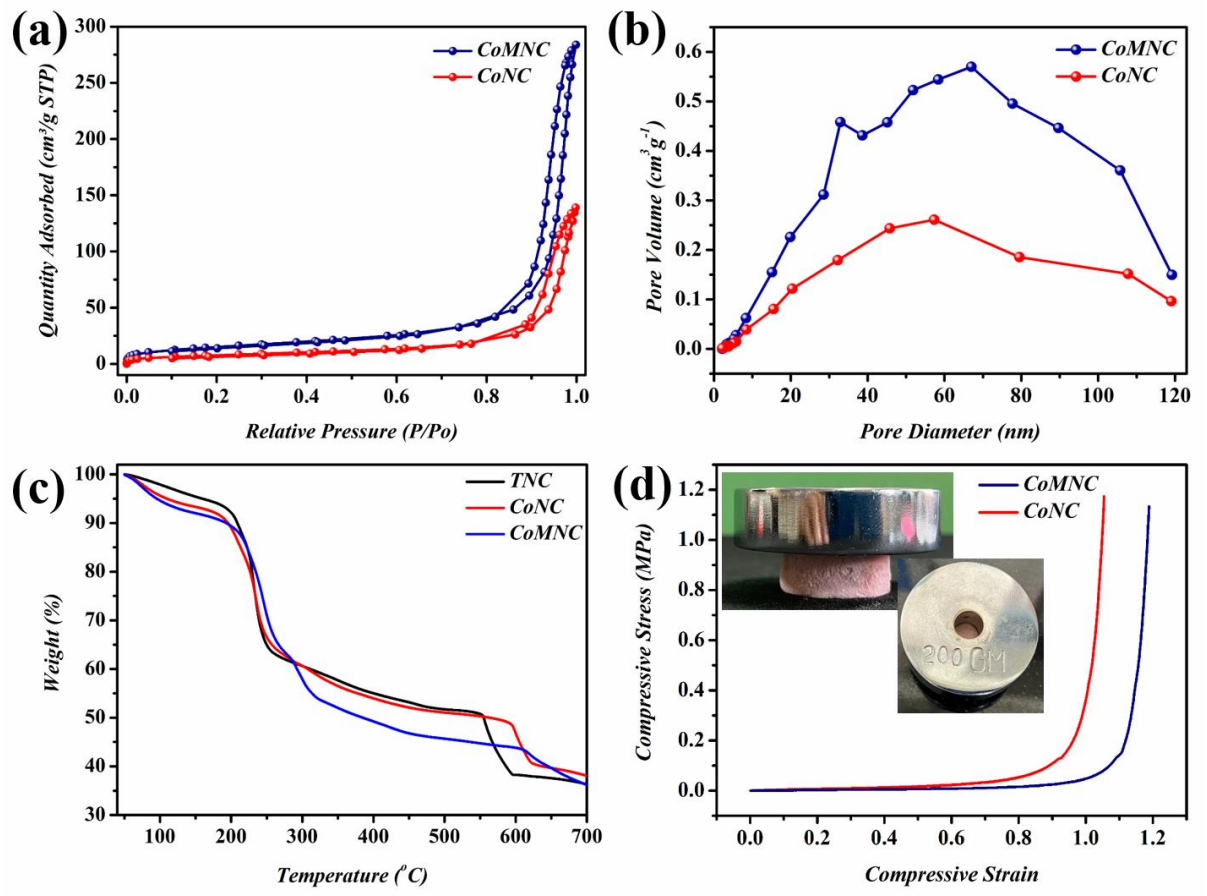

Figure 3. (a) N_2 adsorption−desorption analysis, (b) corresponding BJH pore-size distribution curves, (c) TG curves, and (d) Compression performance of CoNC and CoMNC aerogels.

The inherent and impressive high surface area and light weight of these materials, called aerogels, make them applicable in a variety of industries.

High surface area with light weight is inherent and impressive of these material named aerogels make it applicable in variety of industries. Figure 4a displayed the BET N_2 adsorption-desorption loops for CoMNC and CoNC aerogels. Both curves exhibited typical type II adsorption isotherms with H3 hysteresis loop characteristics of the monolayer-multilayer adsorption.[33] CoMNC aerogels displays considerable variation in BET surface area compared to CoNC aerogels project the highlights of CoMNC aerogel system. CoMNC have a high BET surface area of 88.03 $m^2\ g^{-1}$ straddle that of CoNC aerogel (28.66 $m^2\ g^{-1}$). In BJH pore-size distribution curves (Figure 4b) pore diameters are irregular and distributed in a wide range from minor amount of micro to some macropores which covers the entire mesoporous region as generally observed in nanocellulose based aerogels.[34] When considering the pore volume major fraction of apparent pores were lies in the mesoporous sector having BJH adsorption average pore diameter of 30 nm and 27 nm for CoMNC and CoNC respectively. Considering the previous literature BET surface area mentioned in this report is average for nanocellulose based aerogels and that high values can be achieved by vacuum assisted N_2 adsorption−desorption analysis setup since both aerogels are super sensitive towards the moisture.[35] This high affinity of CoMNC and CoNC aerogels towards water molecules will extensively retard the N_2 adsorption there by actual surface area will be higher than the measured BET surface area. Figure 3c shows the thermal stability of TCNF, CoNC and CoMNC aerogels measured by thermogravimetric analysis (TGA) under air from 50 to 700 °C. Both TCNF and CoNC aerogels exhibited similar thermal behaviours different from CoMNC manifested the change in composition or structure of nanocellulose after the addition of malonic acid that not visible in PXRD. Water absorption nature of aerogels are visible from the initial weight loss (5-8.2%) from 50 to almost 150º C in TGA that shows an increasing trend from TCNF< CoNC< CoMNC. The polymer decomposition stage (about 50% weight loss) starts at about 200 to 350º C followed by subsequent residual substance decomposition stage up to about 600º C.[36] Mechanical properties of CoNC and CoMNC aerogels were studied by compression measurements and the corresponding stress−strain curves are given in Figure 3d. Without shattering of specimen, both CoNC and CoMNC aerogels revealed a buckling to a dense solid film appearance at higher loads. CoMNC shows more improvement in the mechanical properties than CoNC aerogels without forming any fracture or disruption of aerogels offered us the meaningful knowledge about the key role of malonic acid in the nanocellulose/ Co^{2+} cross-linked aerogels.

put comma

put comma

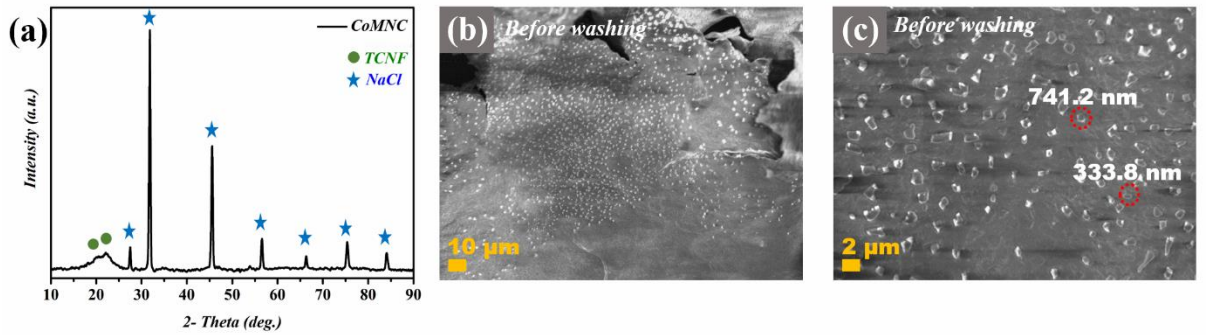

Figure 4. Physical characterization of CoMNC aerogels without washing step before freez drying. a) XRD pattern, b-c) SEM micrographs.

Mechanism of gel formation: Isolation of Cellulose nanofibers (TCNF) was achieved from banana pseudo-stem fibers, agricultural waste through mainly three major intermediate chemical steps; pretreatment by NaOH, bleaching and followed by TEMPO-oxidation. Enormous utilization of Na and Cl contained reagents for these process ultimately leave noticeable amount of Na and Cl in the end product which can be confirmed from the prominent peak of Na KLL in the deconvoluted XPS spectra of TCNF (Figure S3). And it is explicitly known that carboxyl groups created at C6 hydroxyl groups of cellulose chains by TEMPO-oxidation is existing and stable by the interaction between COO^- and Na^+ ions in TCNF. Instant gel formation by addition of salts of metals in to TCNF matrix is fully governed by the complexation interaction between the COO^- groups and metal ions. For example, addition of weak salt like cobalt acetate will promote the instant hydrogelation by coordinating with COO^-, replacing the Na^+ ions in the current position. If the hydrogel formation mechanism is following this pathway, there should be the formation of NaCl as by-product which can remove by purification. Mechanism investigations were done by performing some physical characterisations such as PXRD, SEM and XPS analysis before the purification of samples. Figure 4a displayed the PXRD pattern of CoMNC fabricated without any washing or purification step which shows some extra peaks apart from typical trend of cellulose II originated in the 2ɵ range 27- 85 º compared to PXRD pattern of CoMNC with purification step (Figure 1b). The diffraction peaks precisely recorded at 27.45◦, 31.79◦, 45.54◦, 53.92◦, 56.52º 66.36º 75.38º, and 84.11◦ showed substantial similarity with the typical diffraction pattern of fcc NaCl crystals, which matched to the planes (111), (200), (220), (311), (222), (400), (420) and (422), respectively (JCPDS no. 00-078-0751), confirmed the presence of NaCl crystal formed during the hydrogelation process. These diffraction patterns of NaCl in the aerogel PXRD patterns got eliminated after the proper washing steps leaving behind the XRD

can be removed

diffraction of cellulose II (Figure 2b). This interesting evidence further clarified by capturing surface morphology of CoMNC aerogel layers by SEM before purification. In the SEM micrographs of CoMNC aerogels before purification (Figure 4b-c) we can observe some crystals of several hundred nanometer size were decorated over the aerogel surface reveals the formation of NaCl crystals during the hydrogelation process and these independent crystal can be remove by purifications. XPS survey spectrum also attempted to understand this mechanism of binding efficiency of carboxyl groups to Co^{2+} ions displayed both the presence of Na and Cl elements in the original aerogels, and peak of Cl got vanished after leaving small amount of Na after washing (Figure S4). These results considerable evidence towards the mechanism of gelation and important roles of carboxyl groups in the binding of metal ions.

removed

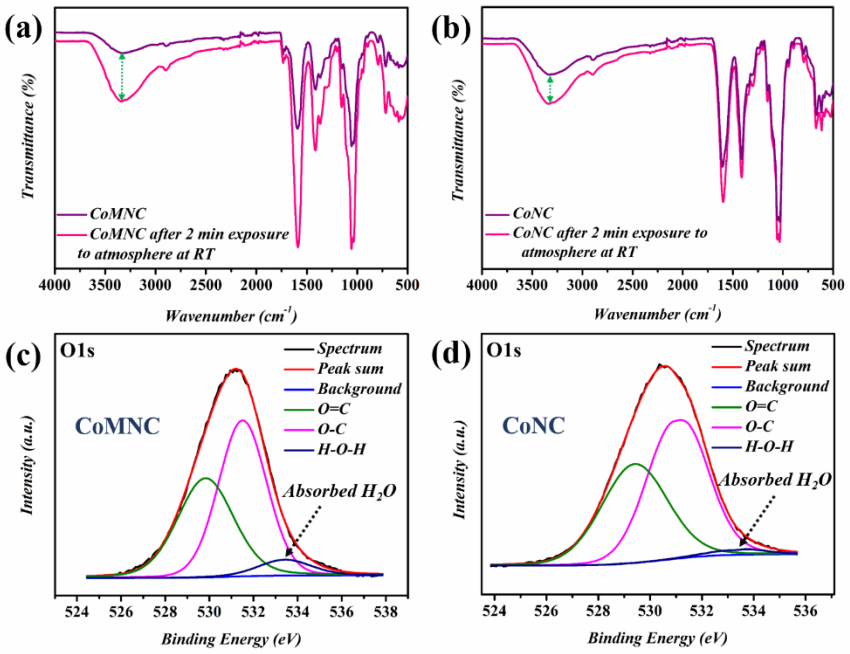

Figure 5. (a-b) FTIR spectra of CoMNC and CONC aerogels after 2 min exposure to atmosphere at room temperature, deconvoluted O1s XPS spectra of (c) CoMNC and (d) CoNC aerogels for humidity absorption rate comparison.

Humidity absorption of aerogels: FTIR measurements CoMNC and CONC aerogels received special attention because both displayed significant change in the intensity of –OH symmetric stretching vibration peak at 3361 cm^{-1} within minutes (Figure 5a-b). This intensification in the –OH stretching is vastly raised and contributed from the absorbed water molecules from the surrounding atmosphere also observed in the deconvoluted O1s XPS spectra of CoMNC aerogels (Figure 5c-d). This explicitly put forward the capability of aerogels absorption of water from moisture or humidity absorption and becomes imperative to study further. For

comparison studies, FTIR spectra measured for both CoMNC and CoNC aerogles at a fixed interval of 2 minutes under room temperature (Figure 5a-b). It has already been witnessed that both showing considerable absorption of atmospheric water whereas CoMNC aerogels achieved more absorption at fixed time of interval resulted in the more positive deviation in the –OH stretching peak intensity. Specific humidity absorption capability of CoMNC aerogels were further manifested from the intensity of peak of absorbed water molecules in the O1s deconvoluted spectra of CoMNC and CONC (Figure 5c-d).

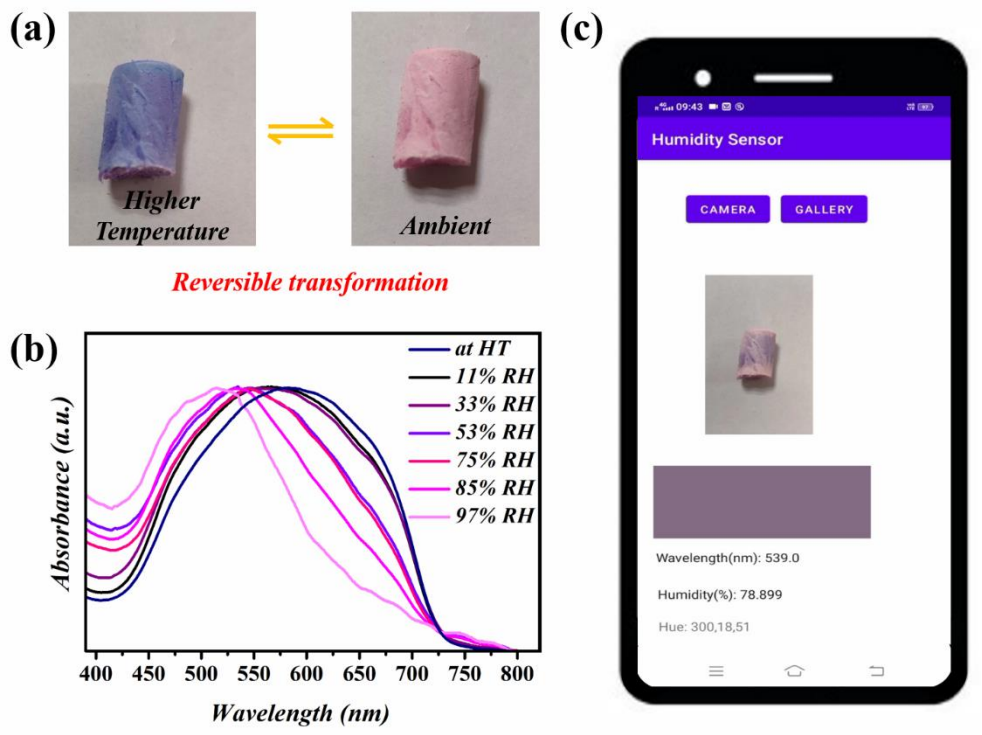

Figure 6. (a) Reversible thermochromism of CoMNC aerogels, (b) UV-Visible absorption spectrum of CoMNC aerogels at different standard humidity, and (d) designed humidity sensor android application with CoMNC aerogels.

It should be (c)

Reversible thermochromism: It is understandable that along with water molecule absorption of CoMNC aerogels there should be a recognisable colour change in the CoMNC aerogels from violet to pink as shown in figure 6a. This allied colour change is exactly resulted from the change in coordination of Co^{2+} coordination from dark coloured tetrahedral to light coloured octahedral by coordinating with water molecules at fifth and sixth coordination valencies. Coordination with water molecules is very weak in the case of CoMNC aerogels and can be removed by keeping it at elevated temperature of about 90ºC for several minutes without harming the structure and humidity absorption properties of aerogels. In fact, our fabricated CoMNC aerogels are highly humidity sensitive and it shows relevant reversible

has

thermochromism. These realizations lead to the applicability of CoMNC towards a naked eye humidity sensing platforms.

Development of humidity sensor: Rate of visible chromic response to the change in humidity was evaluated by monitoring the UV-Visible absorption spectrum at different standard humidity created by the saturated salt solutions (Figure 6b). UV-Visible absorption spectrum was recorded after keeping the CoMNC aerogels in a desiccator contains saturated salt solutions of known humidity for a constant time of 30 sec. Prototype of different humidity surroundings were set in the different glass desiccators by keeping saturated solutions of LiCl, $MgCl_2$, $Mg(NO_3)_2$, NaCl, KCl, and K_2SO_4 solutions, which provide standard and known humidity levels of of 11%, 33%, 53%, 75%, 85%, and 97%, respectively. This time-dependent UV-Vis absorption analysis were repeated with several samples, and found out the accurate and precise λ_{max} at the standard humidity levels. An android application was designed based on these λ_{max} values and corresponding visible light spectrum of colors which enables the digital and easy sensing of humidity without any instruments (Figure 6c). Detailed criteria and steps for the formulation of humidity sensor android application were attached as supplementary information. Since colour change of these Co(II) coordinated malonic acid/nanocellulose hybrid aerogels materials were time dependent, immediate measurements with in one minute is compulsory for the accurate values. This limitation was covered by the android application facility which allow the humidity sensing of pictures of CoMNC aerogels saved in gallery of smart phones captured even long time before. So an instant simple click of a photo of CoMNC aerogels enables sensing of surrounding humidity from your own smart phones at any time. A short time heating of used CoMNC aerogels at 90ºC will make the system active for reuse for further sensing.

CONCLUSIONS

In brief, a reversible thermochromic cobalt(II) coordinated malonic acid/nanocellulose hybrid aerogels by utilizing the synergic action of coordinating power of Co(II) ions and malonic acid assisted cross linking. Induced carboxyl groups from TEMPO-oxidation and handful hydroxy groups played beneficial role in the coordination with Co(II) ions and ester moiety based linkage between fibers by utilizing malonic acid. These cobalt(II) coordinated malonic acid/nanocellulose hybrid aerogels exhibited the intrinsic thermochromic property of Co(II) based materials. Moreover, the fibrous and flexible nature of aerogels with high specific surface area enhanced this phenomenon by reducing the time for these reversible thermochromism

was developed

process. The enhanced reversible thermochromism these hybrid aerogels eluted from its high accessible surface contact with moisture can be utilized as a visible humidity sensor. More specific humidity sensing was enabled by developing an android application for evaluating the colour of aerogels from its spectroscopic absorption characteristics. This sustainable pathway can be ideal for many broad applications that required incorporation of different metal based additives with exciting properties.

ASSOCIATED CONTENT

Supporting Information

The Supporting Information related to this article can be found in the online version.

AFM micrograph and DLS spectra of TCNF; Deconvoluted XPS Co2p spectra of CoNC and CoMNC aerogels; Deconvoluted XPS O1s spectra of TCNF and CoMNC aerogels; XPS survey spectrum of CoMNC aerogels without and with washing step; Android application designing details for humidity sensing based on CoMNC aerogels.

AUTHOR INFORMATION

Corresponding Author

* E-mail: pillai_saju@niist.res.in (S. Pillai)

Notes

The authors do not declare any competing financial interest.

ACKNOWLEDGMENTS

Financial support from the UGC for this research is greatly appreciated.

REFERENCES

1. Thomas, B.; Raj, M. C.; Joy, J.; Moores, A.; Drisko, G. L.; Sanchez, C. m., Nanocellulose, a versatile green platform: from biosources to materials and their applications. *Chemical reviews* **2018,** *118* (24), 11575-11625.
2. Giese, M.; Spengler, M., Cellulose nanocrystals in nanoarchitectonics–towards photonic functional materials. *Molecular Systems Design & Engineering* **2019,** *4* (1), 29-48.
3. Xu, X.; Liu, F.; Jiang, L.; Zhu, J.; Haagenson, D.; Wiesenborn, D. P., Cellulose nanocrystals vs. cellulose nanofibrils: a comparative study on their microstructures and effects as polymer reinforcing agents. *ACS applied materials & interfaces* **2013,** *5* (8), 2999-3009.
4. Hubbe, M. A.; Ferrer, A.; Tyagi, P.; Yin, Y.; Salas, C.; Pal, L.; Rojas, O. J., Nanocellulose in thin films, coatings, and plies for packaging applications: A review. *BioResources* **2017,** *12* (1), 2143-2233.
5. Guccini, V.; Phiri, J.; Trifol, J.; Rissanen, V.; Mousavi, S. M.; Vapaavuori, J.; Tammelin, T.; Maloney, T.; Kontturi, E., Tuning the Porosity, Water Interaction, and Redispersion of Nanocellulose Hydrogels by Osmotic Dehydration. *ACS applied polymer materials* **2021**.

6. Zhu, L.; Zong, L.; Wu, X.; Li, M.; Wang, H.; You, J.; Li, C., Shapeable fibrous aerogels of metal–organic-frameworks templated with nanocellulose for rapid and large-capacity adsorption. *ACS nano* **2018,** *12* (5), 4462-4468.
7. Varghese, H.; Hakkeem, H. M. A.; Chauhan, K.; Thouti, E.; Pillai, S.; Chandran, A., A high-performance flexible triboelectric nanogenerator based on cellulose acetate nanofibers and micropatterned PDMS films as mechanical energy harvester and self-powered vibrational sensor. *Nano Energy* **2022,** *98*, 107339.
8. Ferreira, F. V.; Otoni, C. G.; Kevin, J.; Barud, H. S.; Lona, L. M.; Cranston, E. D.; Rojas, O. J., Porous nanocellulose gels and foams: Breakthrough status in the development of scaffolds for tissue engineering. *Materials Today* **2020,** *37*, 126-141.
9. Isogai, A.; Saito, T.; Fukuzumi, H., TEMPO-oxidized cellulose nanofibers. *nanoscale* **2011,** *3* (1), 71-85.
10. Li, M. C.; Wu, Q.; Moon, R. J.; Hubbe, M. A.; Bortner, M. J., Rheological aspects of cellulose nanomaterials: Governing factors and emerging applications. *Advanced Materials* **2021,** *33* (21), 2006052.
11. (a) Zander, N. E.; Dong, H.; Steele, J.; Grant, J. T., Metal cation cross-linked nanocellulose hydrogels as tissue engineering substrates. *ACS applied materials & interfaces* **2014,** *6* (21), 18502-18510; (b) Hai, J.; Li, T.; Su, J.; Liu, W.; Ju, Y.; Wang, B.; Hou, Y., Anions Reversibly Responsive Luminescent Tb (III) Nanocellulose Complex Hydrogels for Latent Fingerprint Detection and Encryption. *Angew. Chem., Int. Ed* **2018,** *57* (23), 6786-6790.
12. Dong, H.; Snyder, J. F.; Williams, K. S.; Andzelm, J. W., Cation-induced hydrogels of cellulose nanofibrils with tunable moduli. *Biomacromolecules* **2013,** *14* (9), 3338-3345.
13. Cheng, Y.; Zhang, X.; Fang, C.; Chen, J.; Wang, Z., Discoloration mechanism, structures and recent applications of thermochromic materials via different methods: A review. *Journal of Materials Science & Technology* **2018,** *34* (12), 2225-2234.
14. Jaiswal, A. K.; Hokkanen, A.; Kumar, V.; Makela, T.; Harlin, A.; Orelma, H., Thermoresponsive Nanocellulose Films as an Optical Modulation Device: Proof-of-Concept. *ACS Applied Materials & Interfaces* **2021,** *13* (21), 25346-25356.
15. Guo, X.; Kuang, D.; Zhu, Z.; Ding, Y.; Ge, L.; Wu, Z.; Du, B.; Liang, C.; Meng, G.; He, Y., Humidity Sensing by Graphitic Carbon Nitride Nanosheet/TiO2 Nanoparticle/Ti3C2Tx Nanosheet Composites for Monitoring Respiration and Evaluating the Waxing of Fruits. *ACS Applied Nano Materials* **2021,** *4* (10), 11159-11167.
16. Lin, J.; Fang, H.; Tan, X.; Sun, B.; Wang, Z.; Deng, H.; Liu, H.; Tang, Z.; Liao, G.; Shi, T., Ultrafast self-assembly MoS2/Cu (OH) 2 nanowires for highly sensitive gamut humidity detection with an enhanced self-recovery ability. *ACS Applied Materials & Interfaces* **2019,** *11* (49), 46368-46378.
17. Tsigara, A.; Mountrichas, G.; Gatsouli, K.; Nichelatti, A.; Pispas, S.; Madamopoulos, N.; Vainos, N. A.; Du, H.; Roubani-Kalantzopoulou, F., Hybrid polymer/cobalt chloride humidity sensors based on optical diffraction. *Sensors and Actuators B: Chemical* **2007,** *120* (2), 481-486.
18. Zhang, D.; Luo, N.; Xue, Z.; Bai, Y.-L.; Xu, J., Effect of Open Metal Sites in Cobalt-Based Bimetallic Metal–Organic Framework Nanoparticles-Coated Quartz Crystal Microbalance (QCM) for Humidity Detection. *ACS Applied Nano Materials* **2022**.
19. He, X.; Geng, W.; Zhang, B.; Jia, L.; Duan, L.; Zhang, Q., Ultrahigh humidity sensitivity of NaCl-added 3D mesoporous silica KIT-6 and its sensing mechanism. *RSC advances* **2016,** *6* (44), 38391-38398.
20. Zhang, S.; Geng, W.; He, X.; Tu, J.; Ma, M.; Duan, L.; Zhang, Q., Humidity sensing performance of mesoporous CoO (OH) synthesized via one-pot hydrothermal method. *Sensors and Actuators B: Chemical* **2019,** *280*, 46-53.
21. Hakkeem, H. M. A.; Babu, A.; Pal, S. K.; Mohamed, A. P.; Ghosh, S. K.; Pillai, S., Cellulose nanocrystals directed in-situ assembly of Au@ Ag nanostructures with multifunctional activities. *Microchemical Journal* **2021,** *168*, 106393.

22. Zhang, D.; Luo, N.; Xue, Z.; Bai, Y.-L.; Xu, J., Effect of Open Metal Sites in Cobalt-Based Bimetallic Metal–Organic Framework Nanoparticles-Coated Quartz Crystal Microbalance (QCM) for Humidity Detection. *ACS Applied Nano Materials* **2022,** *5* (2), 2147-2155.
23. Nabeela, K.; Thomas, R. T.; Nair, J. B.; Maiti, K. K.; Warrier, K. G. K.; Pillai, S., TEMPO-oxidized nanocellulose fiber-directed stable aqueous suspension of plasmonic flower-like silver nanoconstructs for ultra-trace detection of analytes. *ACS Applied Materials & Interfaces* **2016,** *8* (43), 29242-29251.
24. Zhou, Y.; Saito, T.; Bergström, L.; Isogai, A., Acid-free preparation of cellulose nanocrystals by TEMPO oxidation and subsequent cavitation. *Biomacromolecules* **2018,** *19* (2), 633-639.
25. Allen, T. C.; Cuculo, J. A., Cellulose derivatives containing carboxylic acid groups. *Journal of Polymer Science: Macromolecular Reviews* **1973,** *7* (1), 189-262.
26. (a) Bian, H.; Luo, J.; Wang, R.; Zhou, X.; Ni, S.; Shi, R.; Fang, G.; Dai, H., Recyclable and reusable maleic acid for efficient production of cellulose nanofibrils with stable performance. *ACS Sustainable Chemistry & Engineering* **2019,** *7* (24), 20022-20031; (b) Chen, L.; Zhu, J.; Baez, C.; Kitin, P.; Elder, T., Highly thermal-stable and functional cellulose nanocrystals and nanofibrils produced using fully recyclable organic acids. *Green Chemistry* **2016,** *18* (13), 3835-3843.
27. Yang, C. Q.; Wang, X., Formation of cyclic anhydride intermediates and esterification of cotton cellulose by multifunctional carboxylic acids: An infrared spectroscopy study. *Textile Research Journal* **1996,** *66* (9), 595-603.
28. Benkaddour, A.; Jradi, K.; Robert, S.; Daneault, C., Study of the effect of grafting method on surface polarity of tempo-oxidized nanocellulose using polycaprolactone as the modifying compound: Esterification versus click-chemistry. *Nanomaterials* **2013,** *3* (4), 638-654.
29. Petitto, S.; Langell, M., Surface composition and structure of Co 3 O 4 (110) and the effect of impurity segregation. *Journal of Vacuum Science & Technology A: Vacuum, Surfaces, and Films* **2004,** *22* (4), 1690-1696.
30. Ashok, A.; Kumar, A.; Tarlochan, F., Surface alloying in silver-cobalt through a second wave solution combustion synthesis technique. *Nanomaterials* **2018,** *8* (8), 604.
31. Hakkeem, H. M. A.; Babu, A.; Shilpa, N.; Venugopal, A. A.; Mohamed, A.; Kurungot, S.; Pillai, S., Tailored synthesis of ultra-stable Au@ Pd nanoflowers with enhanced catalytic properties using cellulose nanocrystals. *Carbohydrate Polymers* **2022,** *292*, 119723.
32. Smyrnioti, M.; Ioannides, T., Synthesis of cobalt-based nanomaterials from organic precursors. *Cobalt* **2017,** *49*, 5772.
33. Meng, Y.; Young, T. M.; Liu, P.; Contescu, C. I.; Huang, B.; Wang, S., Ultralight carbon aerogel from nanocellulose as a highly selective oil absorption material. *Cellulose* **2015,** *22* (1), 435-447.
34. Li, Y.; Tanna, V. A.; Zhou, Y.; Winter, H. H.; Watkins, J. J.; Carter, K. R., Nanocellulose aerogels inspired by frozen tofu. *ACS Sustainable Chemistry & Engineering* **2017,** *5* (8), 6387-6391.
35. Cervin, N. T.; Aulin, C.; Larsson, P. T.; Wågberg, L., Ultra porous nanocellulose aerogels as separation medium for mixtures of oil/water liquids. *Cellulose* **2012,** *19* (2), 401-410.
36. Jiang, F.; Hsieh, Y.-L., Cellulose nanofibril aerogels: synergistic improvement of hydrophobicity, strength, and thermal stability via cross-linking with diisocyanate. *ACS applied materials & interfaces* **2017,** *9* (3), 2825-2834.

GRAPHIICAL ABSTRACT